

Can Gemstone Spectral Imaging Accurately Determine the Concentration of Iodine Contrast: A Phantom Study

Le Wang, Bin Liu*, Xing-wang Wu, Jie Wang, Wan-qin Wang, Yong Zhou, Xiao-hong Zhu, Zhang Shuai and Gao Na

Department of Radiology, the First Affiliated Hospital of Anhui Medical University, Hefei, Anhui Province 230022, China

Abstract

Purpose: To assess the accuracy of the quantification of the iodine concentration of contrast agent using gemstone spectral imaging under static and pulsating conditions respectively.

Methods: A phantom with nine test tubes containing iodine contrast in various concentrations (0.4, 0.7, 2.5, 10, 20, 30, 50 and 100 mg/ml) was scanned with gemstone spectral imaging mode of Discovery CT750 HD. All the scans were performed at static and pulsating status at gantry rotation time of 0.6 s, 0.8 s and 1.0 s respectively. Data were transferred to a work station to acquire iodine-based images, and the iodine contrast was measured within same-sized regions of interest at the same level. The relation and discrepancy between measured concentrations and real concentrations of the iodine contrasts were analyzed.

Results: At gantry rotation time of 0.8 s and 1.0 s, either at static status or pulsating status, the measured concentrations were significantly correlated with the real concentrations ($p=0.000$, $r=0.999$), without significant statistic difference ($p>0.05$). However, at gantry rotation time of 0.6 s, there was a statistically significant difference between the measured values and the real values ($p<0.05$), even though existed linear correlation between them ($p=0.000$, $r=0.999$).

Conclusions: Gemstone spectral imaging is a reliable method to accurately quantify the concentration of iodine contrasts, whatever at static or pulsating status at gantry rotation time of 0.8 s and 1.0 s. It therefore can be effectively used in differentiating lesions from normal issues.

Keywords: Spectral imaging; Quantitative analysis; Iodine concentration

Introduction

Conventional CT scan is a kind of Polychromatic X-ray Imaging (TPXI), rather than monochromatic imaging. As we know, polychromaticity of the X-rays causes beam-hardening artifacts in the image and loss of information due to energy averaging [1], which leads to shifts in the CT attenuation values in TPXI scanning. These shifts are unavoidable, causing inaccurate CT attenuation values, which will affect diagnosis. Iterative methods have been proposed to recover the attenuation map under these circumstances [2], but they need more time to be calculated and the speed will be very slow. One way to reduce the occurrence of artifacts and enhance the information content of the scan is to use dual-energy CT scan [3-5]. However, dual-source dual-energy CT imaging only can be used to remove bones and Iodine-water decomposition [6], not to measure the concentrations of materials such as the concentration of contrast. The GSI imaging with rapid kVp switching technique completely changes the conventional CT imaging by obtaining monochromatic images which have the capability to correct beam hardening artifacts and yield a variety of basic materials (such as iodine, water, calcium and so on). It also provides the capability to achieve quantitative measurement, such as the iodine concentration of contrast. This study uses GSI mode to measure iodine concentration of contrast in test tubes and to analyze the accuracy of quantitative measurement in the state of motion and at rest. Quantitative measurement is one of the advantages of this spectral CT, it can provide more information for diagnose.

Materials and Methods

Materials

A standard quantitative dynamic phantom (GE Healthcare China, Beijing) including a polypropylene cylinder with 9 tubes and a power-generated and motion-modified device (Figure 1) was used. The cylinder

had nine cells, eight arranged at intervals of 45° on the circumference and one at the center. Each cell had capability to accommodate one 100 mm long polypropylene tube with an outer diameter of 25 mm, an inner diameter of 18 mm. These test tubes contained different concentrations of a standard iodinated contrast agent (Omnipaque, GE Healthcare) of 0.4, 0.7, 2, 5, 10, 20, 30, 50 and 100 mg/ml (in counter-clockwise order as concentration increased, the highest concentration in the center). The power unit functions as an adjuster of the amplitude and frequency of motion to simulate the body's various motion states (such as breathing, gastrointestinal motility, etc.). An amplitude of



Figure 1: The standard phantom and test tubes.

*Corresponding author: Liu Bin, 218 JiXi Road, Department of Radiology, the First Affiliated Hospital of Anhui Medical University, Hefei, Anhui Province 230022, China, Tel: 13955167161; E-mail: fairy_high@163.com

Received February 19, 2013; Accepted August 26, 2013; Published September 01, 2013

Citation: Wang L, Liu B, Wu XW, Wang J, Wang W, et al. (2013) Can Gemstone Spectral Imaging Accurately Determine the Concentration of Iodine Contrast: A Phantom Study. OMICS J Radiology 2: 141 doi:10.4172/2167-7964.1000141

Copyright: © 2013 Wang L, et al. This is an open-access article distributed under the terms of the Creative Commons Attribution License, which permits unrestricted use, distribution, and reproduction in any medium, provided the original author and source are credited.

± 5 mm and a frequency of 15 beats/min were chosen in this study for simulating the respiratory motion.

Scanning method

The phantom was scanned in GSI mode at rest and in motion respectively using spectral CT (Discovery CT750 HD; GE Healthcare Technologies, Milwaukee, WI). The scanning parameters of GSI mode were as follows: rapid kVp switching between 80 and 140 kVp in 0.5 ms; tube current of 600 mA; slice thickness of 5 mm; slice interval of 5 mm; helical pitch of 0.984; FOV (field of view) of 25 cm; gantry rotation time of 0.6 second, 0.8 second and 1.0 second.

Image processing

Data was transported to AW4.4 workstation and was analyzed with the GSI Viewer (GE Healthcare). Iodine-based image and water-based image were produced on it. On the iodine-based image, we can get the Iodine concentration for any ROI. The iodine concentration of 9 tubes with different concentrations of contrast were measured on iodine-based image with the same size of region of interest (ROI; about 40 mm²). Three regions of interest were selected for each tube, and the average was taken as the iodine concentration. The measurement error between the real iodine concentration and the measured concentration was examined. Comparison was made between the error ratio of each group, using the following equation:

$$\text{error ratio} = |(\text{measured value} - \text{real value})| / \text{real value}.$$

Statistical analysis

All statistical analyses were done with software SPSS 16.0 (Statistical Product and Service Solutions SPSS Inc, Chicago, Ill). The linear regression and paired t-test were used to compare iodine concentration between the measured values and the real values; $p < 0.05$ was considered statistically significant.

Results

1. After GSI scan, different iodine concentrations of contrasts were analyzed at static and pulsating conditions respectively at the iodine-based images (Figure 2). The measured iodine concentrations in each test tube at different gantry rotation time under static and pulsating conditions respectively are given in Table 1. Beam-hardening artifacts caused by Iodine contrast agent were observed under both static and pulsating conditions, and in the pulsating state there were also motion artifacts. Even though various beam hardening artifacts are present in every gantry rotation time, the measured iodine concentration increased when its actual concentration increased.

2. Using linear regression and a paired t-test to analyze the

correlation and the consistency between measured values and real values of iodine concentration at different gantry rotation time the data given in Table 2. At gantry rotation time of 0.8 s and 1.0 s and under static or pulsating conditions, it showed a linear, positive correlation between real values and measured values of the iodine concentration. The paired t-test confirmed that there was no statistical significance between the values, which consequently can be considered as the same. At the gantry rotation time of 0.6 s, measured value and the real values of the iodine concentration were different. However, there was still significant linear correlation between them, and the coefficient was also high ($r = 0.999$).

3. The error ratios for each group are shown in Table 3. At gantry rotation time of 0.8 s and 1.0 s, the error ratios were no more than 20%, regardless of concentration difference and motion status. At gantry rotation time of 0.6 s, the error ratios were less than 18.8% when the iodine concentration of the iodinated contrast agent is higher than 2 mg/ml. However, when the iodine concentration of the iodinated contrast agent is low (0.4 mg/ml and 0.7 mg/ml), the measurement error ratios were high up to 125% regardless of motion status.

Discussion

The conventional CT acquires information on the basis of the hybrid energy, which results in inaccurate CT attenuation values and information loss. In addition, it cannot be used for qualitative decomposition and quantitative measurements. Tissue composition analysis relies on the unique CT attenuation properties of different materials at different tube voltage setting [7]. Energy spectrum CT using single tube of high-low energy rapid switching can effectively resolve this problem. Its tube voltage switches between 80 and 140 kVp during a single rotation; this technique can therefore access two sets of absorption and projection data. As these two sets of data are highly consistent, we can mathematically transform the absorption data into two projection-based sets of material decomposition images that would be needed to generate the measured attenuation, in other words, the attenuation of a material can be represented by the linear combination of two high and low attenuating materials, i.e. basis pair. For example, 1 g bone absorption can be depicted by 0.88 g of water and 0.018 g of iodine. Thus, CT imaging allows the change from single-parameter to multi-parameter imaging, which would potentially offer more information through its capabilities of material decomposition [8], is a giant leap for CT diagnosis [9].

In the experiments detailed here, iodinated contrast agent was mixtures of iodine and water, so the iodine content could be accurately measured from the iodine-based image while the basis pair was iodine and water. It is important to note that material decomposition does not identify materials. On the contrary it determines how much of each material would be needed to produce the observed low and high kVp measurements when two basis materials were given. So the quantitative analysis of the targeted object does not always mean determining the true chemical composition of the object, while iodinated contrast agent we used is a special case.

The effect of motion on the accuracy of iodine concentration determination

During the scanning process, the human body has various types of movement, respiratory motion is the most common one, which produce motion artifacts and presents difficulties for quantitative measurement of CT values. In this study, the amplitude of ± 5 mm and frequency of 15 beats/min were chosen for simulating the motion produce by the human body. The result shows that, at the gantry rotation time of 0.8

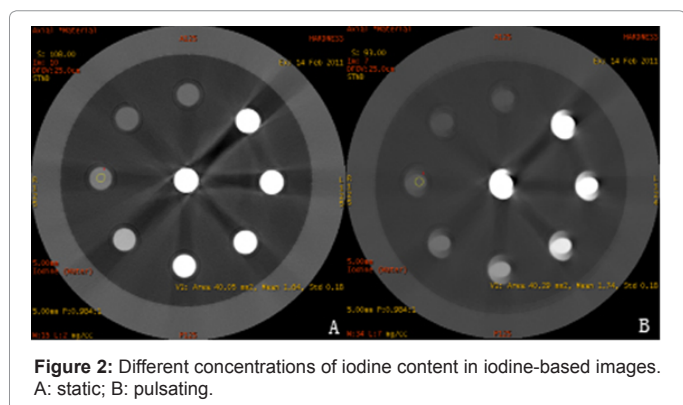


Figure 2: Different concentrations of iodine content in iodine-based images. A: static; B: pulsating.

NO.	Real concentration	Measurement values (at static)			Measurement values (pulsating)		
		0.6s/r	0.8s/r	1.0s/r	0.6s/r	0.8s/r	1.0 s/r
1	0.4	0.90 ± 0.17	0.44 ± 0.19	0.33 ± 0.13	0.77 ± 0.21	0.48 ± 0.17	0.35 ± 0.12
2	0.7	1.22 ± 0.15	0.72 ± 0.17	0.72 ± 0.14	1.13 ± 0.18	0.66 ± 0.15	0.65 ± 0.13
3	2.0	2.25 ± 0.20	1.65 ± 0.19	1.60 ± 0.17	2.09 ± 0.17	1.78 ± 0.16	1.66 ± 0.13
4	5.0	5.60 ± 0.17	4.84 ± 0.16	4.67 ± 0.18	5.38 ± 0.16	4.90 ± 0.16	4.65 ± 0.14
5	10.0	11.88 ± 0.18	10.58 ± 0.14	10.48 ± 0.14	11.66 ± 0.19	10.72 ± 0.15	10.59 ± 0.17
6	20.0	23.10 ± 0.19	21.30 ± 0.19	20.90 ± 0.15	22.72 ± 0.19	21.35 ± 0.17	20.84 ± 0.15
7	30.0	34.40 ± 0.26	31.86 ± 0.25	31.37 ± 0.19	33.50 ± 0.16	31.79 ± 0.22	31.12 ± 0.18
8	50.0	55.34 ± 0.56	51.51 ± 0.40	50.99 ± 0.41	53.42 ± 0.29	50.91 ± 0.34	50.63 ± 0.16
9	100.0	102.17 ± 2.55	95.73 ± 1.47	94.93 ± 1.56	99.02 ± 0.83	96.52 ± 1.81	96.61 ± 1.64

Table 1: The real and measured iodine concentration values for different tube speeds and motion states (mg/ml).

Tube speed		Linear regression		Paired t-test	
		p	r	t	p
static	0.6s/r	0.000	0.999	0.337	0.010
	0.8s/r	0.000	0.999	0.098	0.925
	1.0/s	0.000	0.999	-0.367	0.723
pulsating	0.6s/r	0.000	0.999	2.407	0.043
	0.8s/r	0.000	0.999	0.222	0.830
	1.0s/r	0.000	0.999	-0.249	0.810

At gantry rotation time of 0.8 s and 1.0 s, the real value and measured value of the iodine concentration in the same tube are considered as the same. However, at the gantry rotation time of 0.6 s, there is only linear correlation between them.

Table 2: Relationship between the measured and real values of iodine concentrations.

Real concentration (mg/ml)	Error rate (static)			Error rate (pulsating)		
	0.6s/r	0.8s/r	1.0s/r	0.6s/r	0.8s/r	1.0s/r
0.4	125.00%	10.00%	-17.50%	92.50%	20.00%	-12.50%
0.7	74.28%	2.86%	2.86%	61.43%	-5.71%	-7.14%
2.0	12.50%	-17.50%	-20.00%	4.50%	-11.00%	-17.00%
5.0	12.00%	-3.20%	-6.60%	7.60%	2.00%	7.00%
10.0	18.80%	5.80%	4.80%	16.60%	7.20%	5.90%
20.0	15.50%	6.50%	4.50%	13.60%	6.75%	4.20%
30.0	14.67%	6.20%	4.57%	11.67%	5.97%	3.73%
50.0	10.68%	3.02%	1.98%	6.84%	1.82%	1.26%
100.0	2.17%	-4.27%	-5.07%	-0.98%	-3.48%	-3.39%

At gantry rotation time of 0.8 s and 1.0 s, the error ratios were no more than 20%. Nevertheless, at gantry rotation time of 0.6 s, for low concentrations (0.4 mg/ml and 0.7 mg/ml), the measurement error ratios were high up to 125%.

Table 3: The measurement error rates for different tube speeds under static or pulsating conditions.

s and 1.0 s, the iodine concentration measurements showed positive linear correlation between the real and measured values whether static or pulsating condition is simulated, namely, no statistically significant difference presents between two values. This result means that which meant that, on iodine-based images, the GSI viewer can be effectively used to measure the iodine concentration on the iodine-based images. It also indicated that the accuracy of measurement was not related to low-frequency and low-amplitude motion status.

The effect of gantry rotation times on the accuracy of iodine content determination

There is yet another problem to be considered in clinical work: the selection of the appropriate tube rotation time. Gantry rotation time is closely related to the CT dose index, and reducing the dose is an international research focus [10,11]. The faster the tube rotation, the smaller the radiation dose to the patient, but the more limited is the collected information consequently producing larger measurement

errors). In this study, three different tube rotation times were chosen to simulate the most commonly used mode in clinical practice: 0.6 s, 0.8 s and 1.0 s. At 0.6 s, the iodine concentration measurements showed positive linear correlation between the real values and the measured values, but significant differences existed between these two values. This was possibly caused by the gantry rotation time: the faster the speed of rotation, the more limited the amount of collected data and the higher the background noise.

At gantry rotation times of 0.8 s and 1.0 s, the measured values of iodine concentration were not statistically significantly different from the real values. This indicates that when iodine-based images are adopted, iodine concentration can be measured accurately. As far as the gantry rotation times of 0.8 s and 1.0 s are considered both can accurately reflect the density of the object, but the former gives patients lower dose; thus the gantry rotation time of 0.8 s is recommended for clinical application.

The effect of concentration on the accuracy of iodine content determination

The analysis of the results shows that when the iodine concentrations is low (0.4 mg/ml and 0.7 mg/ml), the gantry rotation time of 0.6 s generates larger errors. Namely, the lower the concentration, the longer rotation time was required for ensuring the accuracy of information. However, further efforts should be made to validate and confirm this observation.

Conclusion

The experimental results show that the spectral CT can be utilized to measure the iodine concentration. When the gantry rotation time of 0.8 s and 1.0 s are adopted, GSI can accurately measure the iodine concentration. However, when the gantry rotation time of 0.6 s is adopted, lager errors under lower concentration will appear.

Similarly, if other basis materials such as calcium-water, calcium-iodine, uric acid-calcium, etc. were used, maybe it will also measure the density of the corresponding basis material composition. This means that the energy spectrum CT brings enormous advancement in material decomposition and quantitative measurements. Whether under static or pulsating conditions, the qualitative measurements showed a high stability. In future, by selecting the correct corresponding basis material, material-based images could be used to accurately reflect the density of a substance, which could be widely applied to all aspects of clinical work.

Spectral CT provides a new way of thinking about CT research [12,13]. However, there are still many problems left unsolved, such as how to select suitable basis materials, what would happen when the chosen basis material and the actual substance composition vary

greatly, how accurate the measurement can be. This is subject to further research and discovery. Moreover, the standard phantom model used in this study could be fairly different from the movement of human organs, and thus its clinical application and the accuracy of the quantitative analysis need to be further confirmed by clinical research and validation.

References

1. Lin XZ, Miao F, Li JY, Dong HP, Shen Y, et al. (2011) High-definition CT Gemstone spectral imaging of the brain: initial results of selecting optimal monochromatic image for beam-hardening artifacts and image noise reduction. *J Comput Assist Tomogr* 35: 294-297.
2. Elbakri IA, Fessler JA (2002) Statistical image reconstruction for polyenergetic X-ray computed tomography. *IEEE Trans Med Imaging* 21: 89-99.
3. Stonestrom JP, Alvarez RE, Macovski A (1981) A framework for spectral artifact corrections in x-ray CT. *IEEE Trans Biomed Eng* 28: 128-141.
4. Sidky EY, Zou Y, Pan X (2004) Impact of polychromatic x-ray sources on helical, cone-beam computed tomography and dual-energy methods. *Phys Med Biol* 49: 2293-2303.
5. Graser A, Johnson TR, Hecht EM, Becker CR, Leidecker C, et al. (2009) Dual-energy CT in patients suspected of having renal masses: can virtual nonenhanced images replace true nonenhanced images? *Radiology* 252: 433-440.
6. Fleischmann D, Boas FE (2011) Computed tomography--old ideas and new technology. *Eur Radiol* 21: 510-517.
7. Gupta RT, Ho LM, Marin D, Boll DT, Barnhart HX, et al. (2010) Dual-energy CT for characterization of adrenal nodules: initial experience. *AJR Am J Roentgenol* 194: 1479-1483.
8. Zhang D, Li X, Liu B (2011) Objective characterization of GE discovery CT750 HD scanner: gemstone spectral imaging mode. *Med Phys* 38: 1178-1188.
9. Rogalla P, Kloeters C, Hein PA (2009) CT technology overview: 64-slice and beyond. *Radiol Clin North Am* 47: 1-11.
10. Mollet NR, Cademartiri F, van Mieghem CA, Runza G, McFadden EP, et al. (2005) High-Resolution Spiral Computed Tomography Coronary Angiography in Patients Referred for Diagnostic Conventional Coronary Angiography. *Circulation*.
11. Raff GL, Gallagher MJ, O'Neill WW, Goldstein JA (2005) Diagnostic accuracy of noninvasive coronary angiography using 64-slice spiral computed tomography. *J Am Coll Cardiol* 46: 552-557.
12. Li Xiaohu, Yu Yongqiang, Wang Wanqin (2011) Composition judgment of in vitro upper urinary calculi: Comparison of gemstone spectral CT and conventional polychromatic X-ray imaging. *Chinese Journal of Medical Imaging Technology*.
13. Fletcher JG, Takahashi N, Hartman R, Guimaraes L, Huprich JE, et al. (2009) Dual-energy and dual-source CT: is there a role in the abdomen and pelvis? *Radiol Clin North Am* 47: 41-57.